Comment on: *Melting behavior of SiO_2 up to 120 GPa* [*Andrault et al.*, 2020]

D. Andrault [1], L. Pison [1], G. Morard [2], G. Garbarino [3], M. Mezouar [3], M.A. Bouhifd [1], T. Kawamoto [4]

[1] Université Clermont Auvergne, CNRS, IRD, OPGC, LMV, Clermont-Ferrand, France
[2] Université Grenoble Alpes, Université, Savoie Mont Blanc, CNRS, IRD, IFSTTAR, ISTerre, 38000 Grenoble, France
[3] European Synchrotron Research Facility, Grenoble, France
[4] Department of Geoscience, Faculty of Science, Shizuoka University, Shizuoka, 422-8529, Japan

I. ABSTRACT

The additional work we have done using our new laser-heating in the diamond anvil cell system since the publication of [*Andrault et al.*, 2020] leads us to the conclusion that there was a systematic bias in the determination of temperature. First, the temperature of the W-lamp used for the calibration of the optical system was overestimated by ~22 K at 2273 K. Then, we made the assumption that hot SiO_2 was a grey-body (constant emissivity $\varepsilon(\lambda)$), while the available measurements suggest instead that $\varepsilon(\lambda)$ of SiO_2 is similar to that of tungsten. Applying these two corrections lowers the SiO_2 melting temperatures significantly. In LMV, we performed a new experimental determination of the SiO_2 melting temperature, at 5000(200) K and ~70(4) GPa, which is well compatible with the amplitude of the correction proposed. The reevaluation of the melting temperature profile does not affect largely the interpretations or the main conclusions presented in [*Andrault et al.*, 2020]. Within the stability field of stishovite, the melting curve still presents a relatively sharp change of slope at P-T recalculated as ~40 GPa and ~4800 K. It is related to a change of the melt structure. At higher pressures, the melting curve is almost flat up to the subsolidus transition from stishovite to the $CaCl_2$-form around 85 GPa, where the slope of the melting curve increases again up to ~120 GPa. We present corrected Figures and Tables of the original publication.

II. CALIBRATION OF THE OPTICAL SYSTEMS

On the course of the development of our new system for laser heating in the diamond anvil cell (LH-DAC) at the *Laboratoire Magma et Volcans* (LMV), we dedicated special efforts to the temperature calibration. Our new LH-DAC system is very similar to that of the ID27 beamline (ESRF), which we used to determine the melting properties of SiO_2 [*Andrault et al.*, 2020]. Both system adopt the basic principles established by us several years ago [*Schultz et al.*, 2005], in particular the Schwarzschild reflective objectives that present no chromatic aberrations [*Giampaoli et al.*, 2018]. The LMV system is optimized for simultaneous temperature measurements on both sides of the sample using the TRax software [*Holtgrewe et al.*, 2019].

Calibration of the optical response of the LH-DAC system is essential for the accuracy of the temperature measurements. At ID27, the same tungsten lamp is used for many years. It presents a flat part on its filament, which achieves a constant temperature (e.g. 2273 K) at a given electric power. The lamp was initially calibrated on a black body reference. The relationship between applied electrical current and W-lamp temperature is checked regularly based on the thermal expansion of W measured using X-ray diffraction [*Miiller and Cezairliyan*, 1990]. With a resolution on the W cell parameter $\Delta d/d$ of ~$1.5\ 10^{-4}$ [*Mezouar et al.*, 2005], the temperature uncertainty is calculated to be ~30-40 K at 2273 K [*Dubrovinsky and Saxena*, 1997; *Miiller and Cezairliyan*, 1990]. Still, there could be other experimental uncertainties than thermal expansion itself.

In LMV, we calibrate the optical response using two techniques: (i) a Pt heating wire is calibrated at 1664 K and 1817 K based melting point of diopside and wollastonite, respectively [*Richet et al.*, 1993]. The onset of melting is indicated by the formation of a thin film of melt at the surface of the wire. Reproducing the measurement several times yields to an uncertainty of <10K. (ii) We acquired a new lamp from Pyrometer-LLC (USA), which thermal emission intensity for photons between 0.6 and 0.7 µm was calibrated on a NIST black body standard at different temperatures between 1973 K and

2573 K. Our two methods of calibration, with Pt-wire and W-lamp, agree with each other within 10-15 K. As a result, we adopted the certified W-lamp at 2273 K to calibrate the optical response of the LMV system. We note that performing the calibration using of a W-lamp implies correcting for the emissivity function ($\varepsilon(\lambda,T)$) of the W-lamp. This is not a negligible effect; a W-lamp at 2273 K presents a thermal emission spectrum similar to a grey-body (constant ε(λ)) at 2358 K (ΔT=-85 K) [*Devos*, 1954].

We then performed a cross-check of the temperature calibration between the LMV and ID27 systems using a secondary W-lamp that was alternately installed on both systems. Its thermal emission spectrum was measured at temperatures between 2244 K and 2566 K using the different optical paths available on both systems. The procedure was repeated after several months. The result is a temperature significantly smaller at LMV compared to ID27, for a same electrical current applied to the W-lamp. The average temperature difference is ~22(14) K in the range of temperature investigated, which is within the uncertainty of the W-lamp temperature based on X-ray diffraction (30-40 K). Such systematic difference does not have major implication for experimental temperatures up to 2500-3000 K, considering that other sources of uncertainties yield to a final temperature uncertainty of ±100 K (see details in [*Andrault et al.*, 2020]). However, it becomes more significant for the study on the melting of SiO_2 that implies temperatures higher than 5000 K.

III. SELECTING A PROPER EMISSIVITY FUNCTION FOR SiO_2

In order to measure the sample temperature properly, one should take into account its $\varepsilon(\lambda,T)$ at high temperature. Unfortunately $\varepsilon(\lambda,T)$ is poorly constrained for SiO_2, which implies making assumptions. In [*Andrault et al.*, 2020], we considered a constant emissivity within the 600-900 nm range of wavelength used for the temperature determination and applied the Wien law to estimate the SiO_2 temperatures. However, an important observation in [*Andrault et al.*, 2020] is a good coupling between the laser radiation at ~1µm and the SiO_2 sample, which is accompanied by a sample darkening in the optical range at 300 K. It makes it unlikely that SiO_2 presents a perfectly flat absorption spectrum of SiO_2 within 600-900 nm at very high temperature. The same property should also apply for the SiO_2 emissivity function, according to the Kirchhoff law correlating to each other these two functions.

Absorption spectra have been reported in the literature for several silicates including SiO_2 [*Trukhin et al.*, 2011] and Fe-bearing bridgmanite (e.g. [*Keppler et al.*, 2008]), even though this range of wavelength is generally not the main region of interest for this type of studies. It is very interesting to note that the absorption spectra present slopes comparable to the emissivity function of tungsten [*Devos*, 1954] within the 600-900 nm range (New Fig. 9). This effect could be due to a stronger interaction between light and electrons with increasing the light energy. This trend favors an alternative assumption to the grey-body (constant ε(λ)); namely a sample $\varepsilon(\lambda,T)$ similar to that of the W-lamp at the calibration temperature of ~2273 K. This hypothesis was largely used in the past in the Mineral Physics community. This implies a significant correction to the SiO_2-sample temperature; e.g. -85 K for a refined grey-body temperature of 2358 K.

IV. CORRECTED RESULTS

We reinvestigate the sample temperatures reported in [*Andrault et al.*, 2020] applying the correction of 22 K to the tungsten lamp and the same $\varepsilon(\lambda,T)$ for SiO_2 and the W-lamp. We are conscious that the latter has consequences; A temperature correction may be applied in the future, when $\varepsilon(\lambda,T)$ of SiO_2 will be better constrained. To calculate the updated sample temperatures (T_{updat}), we consider that the optical response of the ID27 LH-DAC system had not been evaluated properly, considering a W-lamp at 2295 K instead of 2273 K. For a dozen of temperatures between 1500K and 7000K (published temperatures; T_{pub}), we calculate: (i) The grey-body function of the sample at T_{pub}: $GB(T_{pub})$. (ii) The grey-body functions of the W-lamp at 2295 K and 2273 K: $GB(T_{lamp}\text{-old})$ and $GB(T_{lamp}\text{-new})$, respectively. (iii) The sample thermal emission: $TE=GB(T_{pub})*GB(T_{lamp}\text{-new})/GB(T_{lamp}\text{-old})$. (iv) Then, we refine T_{updat} based on TE assuming $\varepsilon(\lambda,T)$ of SiO_2 similar to that of W. The use of Wien or Planck laws is indifferent. It yields a polynomial relation between T_{pub} and T_{updat}: $T_{updat} = -26 + 1.017\ T_{pub} - 2.316\ 10^{-5}\ T_{pub}^2$.

The uncertainty of 14K on the temperature correction of 22(14) K at 2273 K induces uncertainties of 25 or 113 K on the T_{updat} sample temperature at 2816 or 6163 K, respectively. This is significantly smaller than the accuracy of the melting curve temperature determination, which is the temperature difference between data points at which the sample was found solid or liquid (blue and red dots in Fig. 3-corr, respectively).

We reevaluated the sample pressures as well, because we had considered a pressure increase due to some isochoric heating (see [*Andrault et al.*, 2020]). The correction yields significant changes in the melting curve of SiO_2 (Table 1-corr; Fig. 3-corr). For example, the maximum (P,T) investigated are recalculated to be ~117 GPa and ~6200 K, instead of ~120 GPa and ~7000 K in [*Andrault et al.*, 2020].

V. NEW EXPERIMENTAL MEASUREMENT

To check the robustness of the proposed temperature correction, we performed a new determination of the SiO_2 melting temperature using the LH-DAC system of LMV. The sample consisted of two thin pellets of SiO_2 between which we deposited a little bit of Si-powder to facilitate absorption of the ~1 µm laser radiation at low temperature. This is similar as the second series of experiments in [*Andrault et al.*, 2020]. Melting criteria were based on (i) analysis of the relation between the sample temperature and the laser power and (ii) optical observation of the recovered sample (New Fig. 10). For a nominal pressure of 49 GPa (at 300K), temperature increased progressively with laser power until a flattening of this relationship. Above 140 W of laser power, we observed temperature fluctuations because the SiO_2 melt, which was produced sporadically, did not absorb enough laser radiation to maintain the temperature in its stability field. The highest temperature that we could reach up to 180 W is 4950(200) K, which we associate to the highest possible temperature for solid SiO_2 at this pressure. Steady state production of liquid-SiO_2 in this sample (as performed in [*Andrault et al.*, 2020]) would require even more laser power. The sample pressure at ~4950 K is estimated to 70(4) GPa after correction for the thermal pressure. The recovered sample presents circular figures of absorption that are typical of melting corona observed on several types of sample (New Fig. 10).

VI. DISCUSSIONS

Global trends and main conclusions of [*Andrault et al.*, 2020] are not significantly affected by the temperature correction. We detail below the changes that apply:

- The steep SiO_2 melting curve extends to ~40 GPa and the Clapeyron slope between stishovite and the low-density melt (LDM) is ~76 K/GPa (Table 2-corr, New Table 3). This corresponds to similar temperatures than reported in some theoretical calculations [*Belonoshko and Dubrovinsky*, 1995; *Usui and Tsuchiya*, 2010]. On this segment, our data plot more linearly than any other melting studies, including the experimental work [*Shen and Lazor*, 1995]. As mentioned in [*Andrault et al.*, 2020], this observation is compatible with minor changes in the LDM structure up to ~40 GPa.
- The triple point between stishovite, LDM and high-density melt (HDM) is found at ~40 GPa and ~4800 K. We refine a LDM-HDM volume change of -4.21(20) instead of -4.02(20) cm^3/mol in [*Andrault et al.*, 2020].
- A relatively flat melting curve extends from 40 to 85 GPa and 4800 to 5200 K with a Clapeyron slope of 9 GPa/K. The associated stishovite-HDM volume of fusion is 0.56(13) cm^3/mol, which corresponds to 4.0(0.9)% of the stishovite volume. This is ~10 times smaller than the stishovite-LDM volume change of ~4.77 cm^3/mol.
- As a result, the volume change between LDM and HDM melts is ~26%.
- Above 85 GPa, the Clapeyron slope increases again to ~31 GPa/K. At the highest pressure of this study, ~117 GPa, the melting point of SiO_2 in its $CaCl_2$-form plots at ~6200 K, which is just in-between temperatures reported at each side of the solid-liquid transition of shocked quartz [*Akins and Ahrens*, 2002] (Fig. 3-corr).

ACKNOWLEDGEMENTS

We thank P. Asimow, F. Datchi, N. Guignot, J.A. Hernandez, R. Pierru and G. Weck for fruitful discussions about temperature determination based on thermal emission spectra.

REFERENCES

Akins, J. A., and T. J. Ahrens (2002), Dynamic compression of SiO_2: A new interpretation, Geophys. Res. Lett., 29(10), 1394.

Andrault, D., G. Morard, G. Garbarino, M. Mezouar, M. A. Bouhifd, and T. Kawamoto (2020), Melting behavior of SiO_2 up to 120 GPa, Phys. Chem. Mineral., 47(2).

Belonoshko, A. B., and L. S. Dubrovinsky (1995), Molecular-dynamics of stishovite melting, Geochim. Cosmochim. Acta, 59(9), 1883-1889.

Devos, J. C. (1954), A new determination of the emissivity of tungsten ribbon, Physica, 20(9), 690-&.

Dubrovinsky, L. S., and S. K. Saxena (1997), Thermal expansion of periclase (MgO) and tungsten (W) to melting temperatures, Phys. Chem. Mineral., 24(8), 547-550.

Giampaoli, R., I. Kantor, M. Mezouar, S. Boccato, A. D. Rosa, R. Torchio, G. Garbarino, O. Mathon, and S. Pascarelli (2018), Measurement of temperature in the laser heated diamond anvil cell: comparison between reflective and refractive optics, High Pressure Research, 38(3), 250-269.

Holtgrewe, N., E. Greenberg, C. Prescher, V. B. Prakapenka, and A. F. Goncharov (2019), Advanced integrated optical spectroscopy system for diamond anvil cell studies at GSECARS, High Pressure Research, 39(3), 457-470.

Keppler, H., L. S. Dubrovinsky, O. Narygina, and I. Y. Kantor (2008), Optical Absorption and Radiative Thermal Conductivity of Silicate Perovskite to 125 Gigapascals, Science, 322(5907), 1529-1532.

Larrabee, R. D. (1959), Spectral emissivity of tungsten, Journal of the Optical Society of America, 49(6), 619-625.

Mezouar, M., et al. (2005), Development of a new state-of-the-art beamline optimized for monochromatic single-crystal and powder X-ray diffraction under extreme conditions at the ESRF, J. Synchr. Rad., 12, 559-664.

Miiller, A. P., and A. Cezairliyan (1990), Thermal-expansion of tungsten in the range 1500-3600-K by a transient interferometric-technique, International Journal of Thermophysics, 11(4), 619-628.

Richet, P., P. Gillet, A. Pierre, M. A. Bouhifd, I. Daniel, and G. Fiquet (1993), Raman spectroscopy, x-ray diffraction, and phase relationship determinations with a versatile heating cell for measurements up to 3600-K (or 2700-K in air), Journal of Applied Physics, 74(9), 5451-5456.

Schultz, E., et al. (2005), Double-sided laser heating system for in situ high pressure-high temperature monochromatic x-ray diffraction at the ESRF, High Pressure Research, 25(1), 71-83.

Shen, G., and P. Lazor (1995), Measurement of melting temperatures of some minerals under lower mantle conditions, J. Geophys. Res., 100(B9), 17699-17713.

Trukhin, A. N., K. Smits, A. Sharakosky, G. Chikvaidze, T. I. Dyuzheva, and L. M. Lityagina (2011), Luminescence of dense, octahedral structured crystalline silicon dioxide (stishovite), Journal of Luminescence, 131(11), 2273-2278.

Usui, Y., and T. Tsuchiya (2010), Ab Initio Two-Phase Molecular Dynamics on the Melting Curve of SiO_2, J. Earth Sci., 21(5), 801-810.

New Figure 9: **Normalized absorption and emissivity functions**. Emissivity functions of a tungsten wire [*Devos*, 1954; *Larrabee*, 1959] are plotted together with absorption spectra of SiO_2 [*Trukhin et al.*, 2011] and Fe-bearing bridgmanite [*Keppler et al.*, 2008], within the range of wavelength (600-900 nm) used for pyrometric determination of temperature in our LH-DAC experiments.

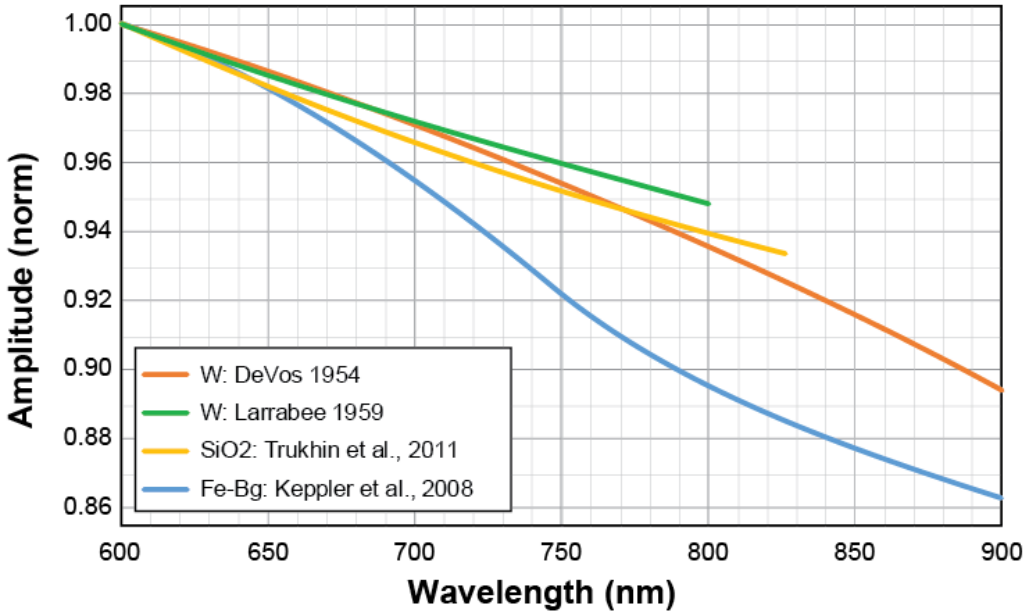

Figure 3 corrected:

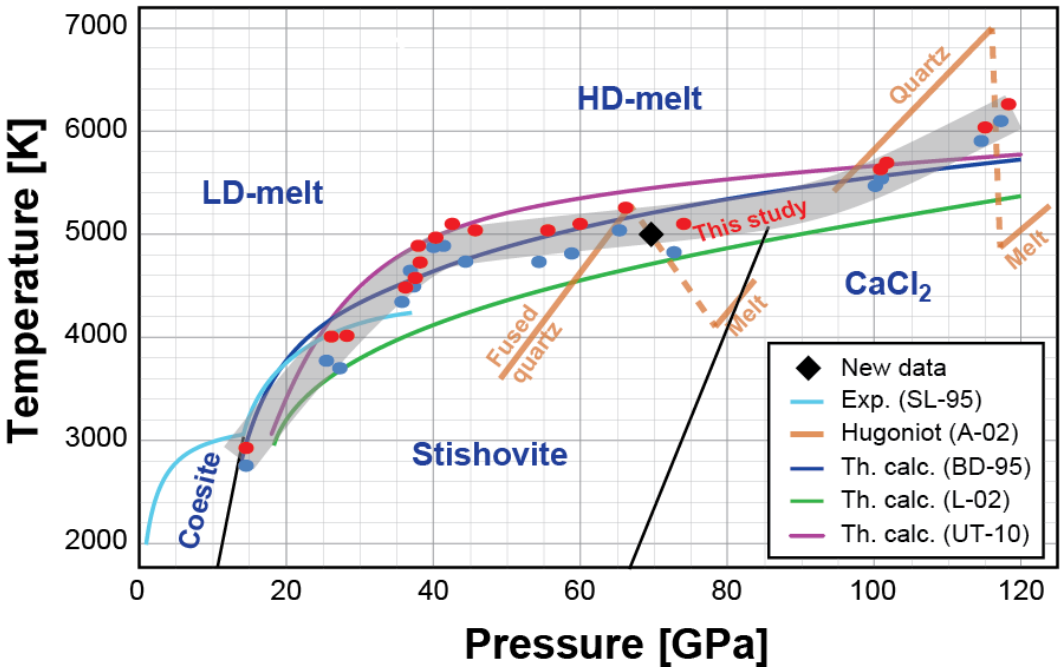

New Figure 10: **(A) Optical microphotograph** showing circular figures around the melted zone of the recovered sample. The external diameter is ~60 µm. (B) **Relationship between sample temperature and laser power**: A maximum temperature of 4950(200) K was reached on both sample sides for a laser power up to 180 W, even though higher temperatures are predicted from the linear relationship between laser power and temperature up to ~120 W (dashed line). Between 140 and 180 W, temperature flucturations occured because the melt, which is produced sporadically at temperatures higher than ~4950 K, does not absorb enough the laser radiation to maintain the sample temperature in its stability field (AV for front side and AR for rear side of the sample).

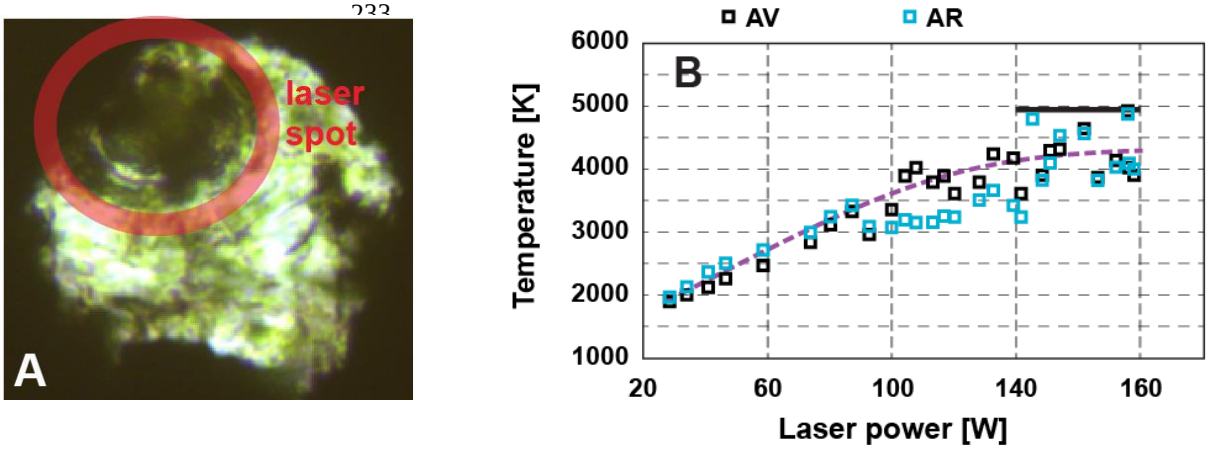

Table 1 corrected:

P(300K) GPa	Temp. K	P(high-T) GPa	Temp solid	Temp Melt
12	2816	14	2728	2904
16	3877	25	3754	4000
19	3836	28	3671	4000
19	4751	37	4636	4866
19.5	4713	37	4519	4713
20	4866	40	4866	4942
21	4942	42	4866	5093
21.5	4558	38	4479	4713
21.5	4401	36	4321	4479
26	4866	46	4713	5018
36	4866	55	4713	5018
39	5018	60	4790	5093
45	5093	66	5018	5241
54	5018	74	4790	5093
76	5605	102	5533	5676
76	5533	101	5461	5605
85	6163	117	6095	6231
85	5957	114	5888	6026

Table 2 corrected:

Transition considered	**Press.** GPa	**Temp.** K	**dT/dP** K/GPa	**ΔS** mol/K	**ΔV** cm3/mol	**Vstish** cm3/mol	**Vcoes** cm3/mol	**VLDM** cm3/mol	**VHDM** cm3/mol	**ΔV/V**
C => S	15	2900	312 a	-15.3 a	-4.77 b	14.69 g	19.46 h			-28% k
C => LDM	15	2900		74.9 d	0.00 e		19.46 h			
S => LDM	15	2900	76 *	62.7 b	4.77 g	14.69 g		19.5 i		28% k
S => HDM	40	4800	9 *	77.7 d	0.69 b	13.63 g			14.3 j	4.9% k
LDM=>HDM	40	4800		-15.0 c	-4.08 f			18.4 i	14.3 j	-25% k
S => HDM	40	4800	9 *	62.7 d	0.56 b	13.63 g			14.2 j	4.0% k
LDM=>HDM	40	4800		0.0 c	-4.21 f			18.4 i	14.2 j	-26% k
S => HDM	40	4800	9 *	47.7 d	0.42 b	13.63 g			14.1 j	3.1% k
LDM=>HDM	40	4800		15.0 c	-4.34 f			18.4 i	14.1 j	-27% k

C, S, LDM and HDM stand for Coesite, Stishovite, low-density and high-density SiO2 melts
*, this study
a, from Akaogi et al. (2011)
b, calculated based on the Clapeyron relation dT/dP=ΔV/ΔS
c, value assumed to be -15, 0 or 15 J/molK (see text)
d, derived from Clapeyron relations around the (C, S, LDM) or (C, LDM, HDM) triple points
e, derived from the flat melting curve of coesite between 9 and 14 GPa (Zhang et al., 1993)
f, calculated using ΔV=VHDM-VLDM
g, calculated at the considered P-T conditions using the EoS of Wang et al. (2012)
h, calculated using Vcoes=Vsti+ΔV(C-S)
i, calculated using VLDM=Vsti+ΔV(LDM-S)
j, calculated using VHDM=Vsti+ΔV(HDM-S)
k, ΔV of the transition normalized to the mean value between the two phases considered

New Table 3: Conditions (P-T) of the triple points and maximum conditions performed in this study. We also report the Clapeyron slopes between these points taken 2 by 2.

	Pressure GPa	Temperature K	Slope K/GPa
Triple (C,S,LDM)	15	2900	
Triple (S,LDM,HDM)	40	4800	76
Triple (S,CaCl2,HDM)	85	5200	9
P-T max	117	6200	31